Viscoelastic characterization of seven laminated glass interlayer materials from static tests

Xavier Centelles[1], Fernández Pelayo[2], María Jesús Lamela-Rey[2], A. Inés Fernández[3], Rebeca Salgado-Pizarro[3], J. Ramon Castro[1], Luisa F. Cabeza[1,*]

[1] GREiA Research Group, University of Lleida, Pere de Cabrera s/n, 25001, Lleida, Spain

[2] Department of Construction and Manufacturing Engineering, University of Oviedo, Campus de Gijón, Zona Oeste, Edificio 7, 33203, Gijón, Spain

[3] Department of Materials Science and Physical Chemistry, Universitat de Barcelona, Martí i Franqués 1-11, 08029, Barcelona, Spain

*Corresponding author: Tel: +34 973003576. Email: luisaf.cabeza@udl.cat

Abstract

The mechanical behaviour of laminated glass is strongly affected by the polymeric interlayer placed between glass layers. In general, this interlayer is a viscoelastic material, and therefore it may experience creep and stress relaxation when subjected for an extended period to a constant stress or strain respectively. In this study, seven different commercial interlayer materials (EVALAM, EVASAFE, PVB BG-R20, Saflex DG-41, PVB ES, SentryGlas, and TPU) were evaluated with relaxation tests at different temperatures, in order to build the relaxation master curves through the time-temperature superposition principle. A generalized Maxwell model was chosen to describe the viscoelastic behaviour of the tested materials. This paper includes the coefficients of the Prony series that fit better the experimental results. This paper has two main goals. First, to present the Prony coefficients (e_i and τ_i), which can then be used to create numerical models that take into consideration the time and temperature-dependant behaviour of the interlayer. Second, to provide the two components of the complex modulus ($E^*(\omega)$) of each material, the storage modulus ($E'(\omega)$) and the loss modulus ($E''(\omega)$), which can be obtained from the relaxation modulus ($E(t)$) by using analytical interconversions.

Keywords: Polymeric interlayer; Laminated glass; Generalized Maxwell model; Prony series; stress relaxation tests

1. Introduction

1.1. Viscoelastic interlayers in laminated glass

The right understanding and use of construction materials entailed remarkable improvements in the execution of singular buildings. A common characteristic among them, regardless of its location, use, and shape, is that they have abundant sunlight and a high transparency. The use of glass evolved and expanded from windows to glazed facades and roofs. Glazing elements became safer with the use of laminated glass, in which two or more glass layers are bonded using a polymeric interlayer that prevents glass shards from scattering in case of accidental breakage. More recently, buildings from the twenty-first century started using laminated glass as a structural material in beams, columns, and staircases, among others. Such a demanding use of laminated glass requires a thorough knowledge of its mechanical behaviour.

The shear behaviour of the interlayer material affects the deformability and the load-bearing capacity of laminated glass plates [1], as well as its post-breakage behaviour [2-4]. In other words, the polymeric interlayer governs the general behaviour of laminated glass; hence, its importance for an adequate design and calculation of laminated glass structural elements. Interlayer materials are viscoelastic, which means that their stiffness and mechanical response depends on the load duration and working temperature [5-7]. Therefore, the mechanical properties of laminated glass also depend, at least, on these two factors [1,8,9].

1.2. Mechanical characterization of viscoelastic materials

The time and temperature variables play a key role in the viscoelastic response of polymers. The mechanical behaviour of viscoelastic materials is a combination of an elastic behaviour, where the stress is proportional to the strain, ruled by the Hooke law ($\sigma_e = E \cdot \varepsilon_e$), and a viscous behaviour, where the stress is proportional to the strain rate, ruled by the Newton law ($\sigma_v = \eta \cdot d\varepsilon_v/dt$).

Ranocchiai et al. [10] reviewed the different test methods to determine of the dynamic properties of polymeric interlayers in laminated glass according to the current standards. Tests to characterize viscoelastic materials can be either static or dynamic. In static tests, the strain rate is either zero or moderate and constant. Static tests include, but are not limited to: creep tests, in which a constant stress is applied in order to see the evolution of the strain over time, and stress relaxation tests, in which a constant strain is applied in order to see the evolution of the response

of the material (i.e., stress) over time. Instead, a mechanical test is considered to be dynamic when either the applied deflection or the measured stress experience variations over time (e.g., sinusoidal oscillations). The properties of viscoelastic materials in dynamic tests may be affected by viscosity effects as the strain rate or frequency increase.

Figure 1 shows the mechanical response over time of a viscoelastic material under constant stress. When a viscoelastic material is subjected to a constant stress (σ_0), it has an instantaneous elastic strain (ε_e), and a gradually increasing viscous strain (ε_v), known as creep. When the stress is removed, there is also an instantaneous elastic recovery and a progressive viscous recovery. The higher the viscous component of the material, the higher the time-dependency of the response. If the material is viscoplastic, it will also have a permanent plastic strain (ε_p).

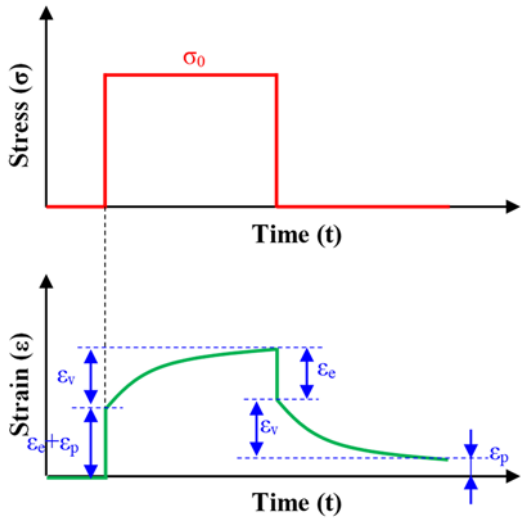

Figure 1. Instantaneous deformation, creep and recovery experienced by a viscoelastic material under a constant stress in a static test.

Figure 2 shows another type of static tests, where a viscoelastic material is subjected to constant strain (ε_0). The material has an initial elastic response (σ_0), but that stress gradually decreases with time due to stress relaxation.

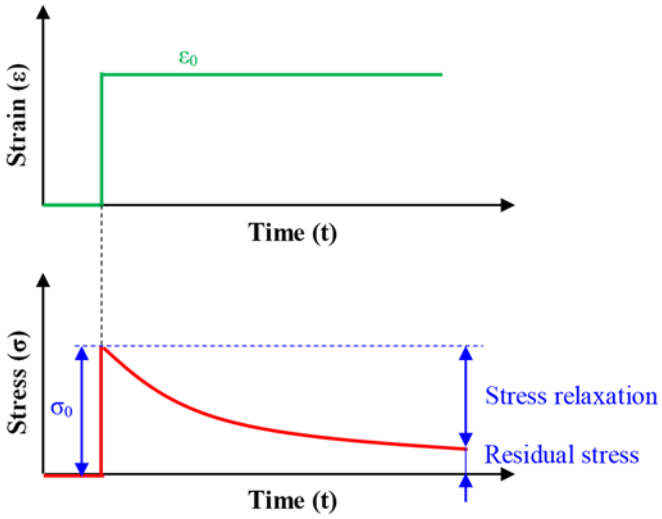

Figure 2. Stress relaxation experienced by a viscoelastic material under a constant strain in a static test.

Figure 3 shows an illustration of a dynamic test, where a sinusoidal stress is applied. The material response is a sinusoidal strain. The amplitude of the response (ε_0) is proportional to the amplitude of the applied stress (σ_0). There is a temporal offset δ between the applied stress and the strain response. The phase angle is higher in materials in which the viscous component is predominant, and lower in materials with a closer to elastic mechanical behaviour.

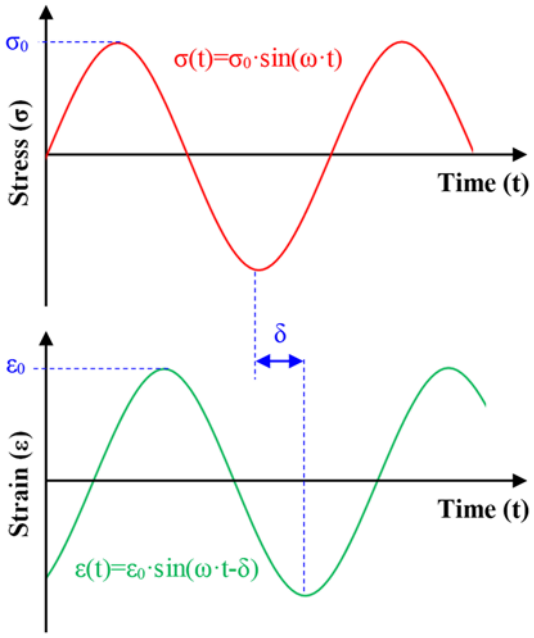

Figure 3. Mechanical response of a viscoelastic material under an oscillatory load.

The dynamic response of viscoelastic materials can be described with the complex modulus as a function of the applied stress frequency (E*(ω)). It can also be represented with the storage modulus (E'(ω)) and the loss modulus (E''(ω)). E'(ω) is associated to the elastic strain energy

stored in the material when a dynamic stress is applied, whereas E''(ω) is associated to the energy that is dissipated by the material when a dynamic stress is applied. The previously mentioned temporal offset between the applied stress and the strain response can also be represented by the phase angle tan(δ)=E''/E'.

The storage modulus relates the stress in phase with the strain, whereas the loss modulus relates the stress in phase with the strain rate, which has a 90º offset with respect to the strain (in the case, for example, of a sinusoidal load). That is why the complex modulus can be displayed in the complex plane (Eq. 1), being E'(ω) the real part and E''(ω) the imaginary part, forming a 90º angle between both.

$$E^*(\omega) = E'(\omega) + iE''(\omega) \qquad \text{Eq. 1}$$

The temperature affects the mobility between the polymer chains, and therefore the polymer stiffness. For temperatures below the glass transition temperature (T_g) the material has a predominantly glasslike consistency, whereas above T_g it has a rubberlike consistency. In the region near T_g, the material is highly time- and frequency-dependent, whereas at both ends ($T >> T_g$ and $T << T_g$) the material is less sensitive to these two parameters [11].

The time also affects the behaviour of viscoelastic materials. As previously indicated, the amount of creep [8] or stress relaxation [12] experienced by a material under a constant stress or strain respectively depend on time, as well as the polymer chain structure and temperature.

In those rheological simple viscoelastic materials, changing the test temperature shifts the E(t) curve on the time logarithmic scale on a quantity depending on the temperature variation (if the change in density is neglected). This correlation is known as the time-temperature superposition (TTS) principle [11].

The TTS models allows to obtain the correlation coefficients, known as shift factors, a_T, which establish a correlation between the relaxation time (t) at a given temperature (T) and the equivalent relaxation time (t/a_T) at a chosen reference temperature (T_0). Such correlation is presented in Eq. 2 for static modules, and Eq. 3 and Eq. 4 for dynamic modules. To obtain the shift factor, the Williams, Landel and Ferry (WLF) TTS model [13] is frequently used. The value of a_T in the WLF equation is obtained using Eq. 5, where C_1 and C_2 are the WLF constants, which depend on the original temperature (T), the reference temperature (T_0), and the glass transition temperature (T_g).

$$E(t,T) = E(t/a_T, T_0) \quad \text{Eq. 2}$$

$$E'(\omega,T) = E'(a_T \cdot \omega, T_0) \quad \text{Eq. 3}$$

$$E''(\omega,T) = E''(a_T \cdot \omega, T_0) \quad \text{Eq. 4}$$

$$\log(a_T) = \frac{-C_1(T-T_0)}{C_2 + (T-T_0)} \quad \text{Eq. 5}$$

The TTS principle can be used, for example, to obtain information for the behaviour of a material on a wider time domain, by shifting horizontally the E(t) from the tested temperature to the reference temperature T_0 (Figure 4), using the shift factors a_T [13]. If the original curves overlap over a certain range (Figure 5), it is possible to perform the time-temperature shifting with the Closed-Form-Shifting (CFS) algorithm presented by Gergesova et al. [14]. For its technical rigor, this mathematical procedure has been adopted as normative [15], although it is only applicable for the complex modulus.

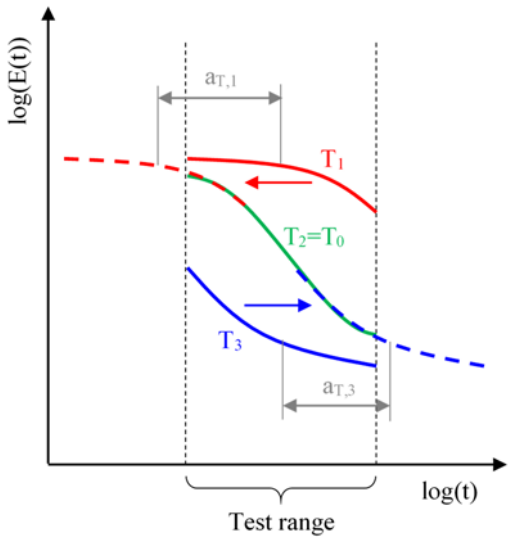

Figure 4. Horizontal shifting of the relaxation curves at different temperatures to match with the curve at the reference temperature T_0.

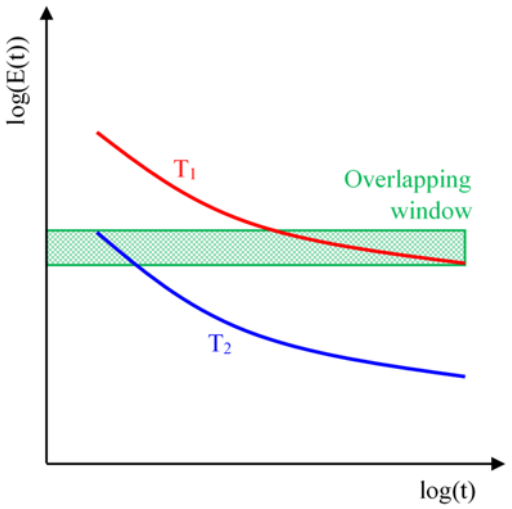

Figure 5. Overlapping window between the relaxation curves at two different temperatures.

Static tests allow obtaining the master curve of the relaxation modulus E(t) for each testing temperature. That master curve has a horizontal asymptote at short load duration time, referred to as instantaneous modulus or E_0, and another at long load duration time, referred to as equilibrium modulus or E_∞ (Figure 6).

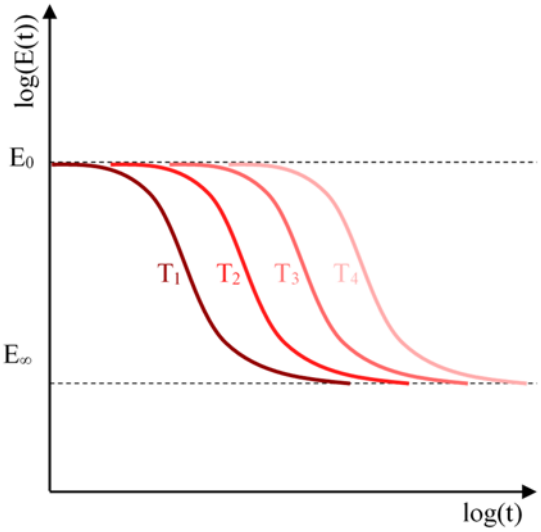

Figure 6. Relaxation master curves at different reference temperatures.

1.3. Analytical models for viscoelastic materials

There are several models aiming to describe viscoelasticity, based on combinations of springs, governed by the Hooke law (Eq. 6), and dashpots, governed by the Newton law (Eq. 7). The Maxwell model and the Kelvin-Voigt model are two of the most basic ones. The Maxwell model has a spring and a dashpot connected in series, and the Kelvin-Voigt model has a spring and a

dashpot connected in parallel. The Maxwell and the Kelvin-Voigt models can be represented with the mathematical expressions from equations 8 and 9, respectively, where σ_e represents the elastic stress, ε_e the elastic strain, E the Young modulus, σ_v the viscous stress, ε_v the viscous strain, and η the viscosity:

$$\sigma_e = E \cdot \varepsilon_e \quad \text{Eq. 6}$$

$$\sigma_v = \eta \cdot d\varepsilon_v/dt \quad \text{Eq. 7}$$

$$\frac{d\varepsilon}{dt} = \frac{1}{E} \cdot \frac{d\sigma}{dt} + \frac{1}{\eta} \cdot \sigma \quad \text{Eq. 8}$$

$$\sigma = E \cdot \varepsilon + \eta \cdot \frac{d\varepsilon}{dt} \quad \text{Eq. 9}$$

The generalized Maxwell model is obtained by connecting several Maxwell elements in parallel. It can be represented by a Prony series as shown in Eq. 10, where E_0 is the instantaneous modulus, n is the number of Maxwell elements connected in parallel, and e_i and τ_i are the Prony coefficients. Although the dynamic complex modulus master curve can be obtained by performing dynamic tests on viscoelastic materials, its real and complex components can also be obtained from static tests using interconversion methods [16]. As an example, with the relaxation modulus E(t) in terms of the Prony coefficients e_i and the characteristic relaxation time coefficients τ_i, it is possible to obtain the storage modulus E'(ω) (Eq. 11) and the loss modulus E''(ω) (Eq. 12) by using interconversion methods [6,16,17], i.e. with Equations 11 and 12.

$$E(t) = E_0 \left[1 - \sum_{i=1}^{n} e_i \left(1 - \exp\left(-\frac{t}{\tau_i}\right)\right)\right] \quad \text{Eq. 10}$$

$$E'(\omega) = E_\infty + \sum_{i=1}^{n} \frac{\tau_i^2 \omega^2 e_i}{\tau_i^2 \omega^2 + 1} \quad \text{Eq. 11}$$

$$E''(\omega) = \sum_{i=1}^{n} \frac{\tau_i^2 \omega^2 e_i}{\tau_i^2 \omega^2 + 1} \quad \text{Eq. 12}$$

1.4. Objectives

The main goal of this paper is to make a viscoelastic characterization of seven different interlayer materials, analysing the results and comparing the different materials. To do the viscoelastic characterization, each material is subjected to relaxation tests at different temperatures. From the relaxation curves at different temperatures, it was possible to represent the relaxation master curve using the time-temperature superposition principle [13] and the t-T-P shifting (CFS) algorithm [14]. From the relaxation tests it was also possible to plot the dynamic master curves: the storage

(E'(ω)) and loss (E''(ω)) moduli, as well as the offset angle (tan(δ)) by using interconversion methods [6,16,17].

It is important to highlight that the tests were performed on polymeric films alone (i.e., not adhered to glass). During the lamination procedure to create the bond between glass and interlayer, laminated glass is exposed to high pressure and temperature in the autoclave, which may affect the mechanical properties of the interlayer [5].

2. Materials

There are several polymers used as interlayer materials for laminated glass. The most common ones are polyvinyl butyral (PVB), ionomers (e.g. SentryGlas), polyethylene-co-vinyl acetate (EVA), and thermoplastic polyurethane (TPU) [18]. PVB was the first polymer used as interlayer material for laminated glass. It was initially used in car windshields [19], but its application soon expanded to glazing systems [20]. It was originally manufactured by DuPont, and nowadays it is commercialised by Kuraray Group, Eastman and Sekisui.

PVB was the first interlayer material to be used in laminated glass, and it is still widely used for architectural applications. For these reasons, it is the most studied and discussed in the literature. Different authors did a viscoelastic characterization of PVB [5-7]. However, several other interlayer materials are being developed for many specific applications. That includes stiffer interlayers for structural applications (e.g. SentryGlas, Saflex DG-41, and PVB ES) [4,21], interlayers for PV modules and other applications that require no autoclave (e.g. EVASAFE or EVALAM) [22], and interlayers that can bond to both glass and stiff polymers such as polycarbonate (PC) or polymethylmetacrilate (PMMA) for safety and security glazing (e.g. TPU) [23].

EVALAM is supplied by Pujol [24]. It is a polyethylene-co-vinyl acetate (EVA), which is a copolymer of ethylene and vinyl acetate. According to the manufacturer, it has a higher transparency and better adhesion with glass than standard PVB. EVASAFE is also an EVA based polymer, which is supplied by Bridgestone [25]. The main difference between EVASAFE and EVALAM is the percentage of vinyl acetate (VA) and ethylene in each of them. The percentage of VA usually varies from 10 wt% to 40 wt%, being softer and more elastic with a higher percentage of VA [18]. According to the manufacturer [25], EVASAFE has a higher strength and stiffness than EVALAM, and therefore a lower percentage of VA.

PVB BG-R20 is a PVB commercialised by Kuraray [26] widely used for automotive and architectural applications. PVB ES is also a PVB commercialised by Kuraray [26], but it has a lower amount of plasticiser than PVB BG-R20. The plasticiser increases the mobility between polymer chains, which means that PVB becomes stiffer by reducing the amount of plasticiser. By increasing the amount of plasticiser, the glass transition temperature decreases. Therefore, PVB ES is stiffer and has a higher glass transition temperature than PVB BG-R20, and it is more adequate for applications where a higher pre- or post-breakage strength and stiffness are required. Saflex DG-41 is commercialised by Eastman [27]. It is also a PVB with a lower amount of plasticiser than PVB BG-R20, and has similar mechanical properties to PVB ES.

SentryGlas is a ionomer, which is classified in the group of thermoplastics. It presents a higher stiffness than standard PVB, as well as a high transparency and a very good adhesion to both glass and steel, which make it a very good alternative to PVB for structural applications [28] and laminated glass elements with embedded metallic joints [29]. Because of its high stiffness and strength, it is also used in hurricane glazing [30]. SentryGlas is manufactured by DuPont and commercialised by Kuraray [26].

Thermoplastic polyurethane (TPU) is a copolymer that combines soft segments, which make it more ductile, with glassy segments, which make it stiffer. TPU is often used in hybrid components of glass and PC or PMMA layers, because of its excellent adhesion capacity to both substrates.

The seven polymeric interlayers chosen for this test are the same ones previously tested by Centelles et al. [31] through uniaxial tensile tests until breakage. On that occasion the effect of previous exposure to accelerated ageing tests was also taken into consideration.

3. Methodology

In order to proceed with the mechanical characterization of the different polymers included in this study, relaxation tests were carried out in a dynamic mechanical thermal analyser DMTA equipment (RSA3 TA Instruments) using the clamps for tensile tests (Figure 7). The specimens have a length of 30 mm, and variable thickness depending on the interlayer material (Table 1). The width of the specimens ranged between 5 mm for stiffer specimens and 10 mm for softer specimens. That variation was made in order to avoid excessively high loads for thick interlayers, which could surpass the limit of the load cell (35 N), and low loads for soft interlayers, which would affect the accuracy of the results if the load cell was not sensitive enough.

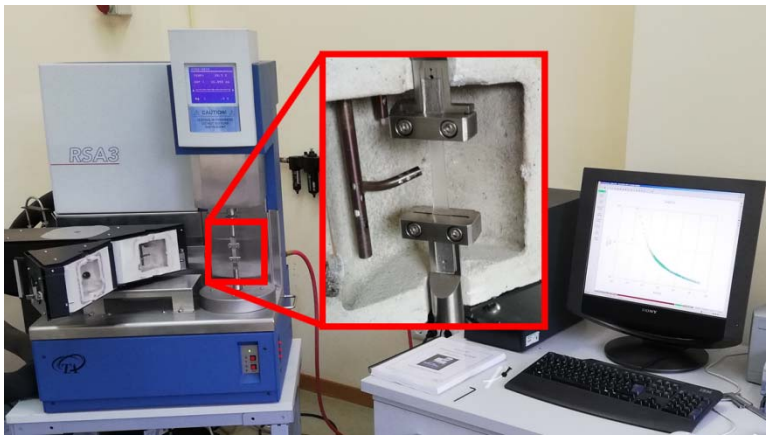

Figure 7. DMA RSA3 by T.A. Instruments. Test setup and clamp detail. Equipment at the University of Oviedo.

Table 1. Thickness of the tested polymeric films.

Interlayer material	**Thickness**
EVALAM	0.38 mm
EVASAFE	0.38 mm
PVB BG-R20	0.76 mm
Saflex DG-41	0.76 mm
PVB ES	0.76 mm
SentryGlas	0.89 mm
TPU	0.13 mm

In order to obtain the master curve for each material, several relaxation tests at 1% constant strain level were carried out with a duration between two and three minutes each (depending on the material) and at different temperatures. The temperature ranged from -10 ºC to 50 ºC, for all interlayer materials. This temperature range was chosen considering that it was a typical one for laminated glass in buildings. Additionally, in the case of SentryGlas, the experimental relaxation curves were extended to 70 ºC. This exception in SentryGlas was made in order to include the glass transition region, which is higher in this material according to the literature [18,26]. The master curves were obtained by applying the CFS algorithm to the experimental data, and the resulting curves were smoothed by a cubic spline interpolation.

The tests at different temperatures were all conducted on the same specimen, in order to ensure that the specimen dimensions, clamp pressure, and other test factors which could distort the results were the same. For each interlayer material, the first test was at the lowest temperature, and then it kept increasing gradually until reaching the highest temperature. Between tests, there was a time lapse of at least five minutes to allow the specimen to recover the deformation and increase

its temperature. Each test was repeated in order to ensure that the specimen had reached the new test temperature.

4. Results and discussion

The relaxation curves, $E(t)$, obtained from the experiments at different temperatures are presented in Figure 8 for EVALAM, EVASAFE, PVB BG-R20, Saflex DG-41, PVB ES, and TPU, and in Figure 9 for SentryGlas. They are presented in different figures to highlight that the temperature range was different for SentryGlas than for the other six materials as was mentioned before. On the other hand, both figures 8 and 9 are in the same scale in order to simplify the comparisons between the materials behaviour with temperature.

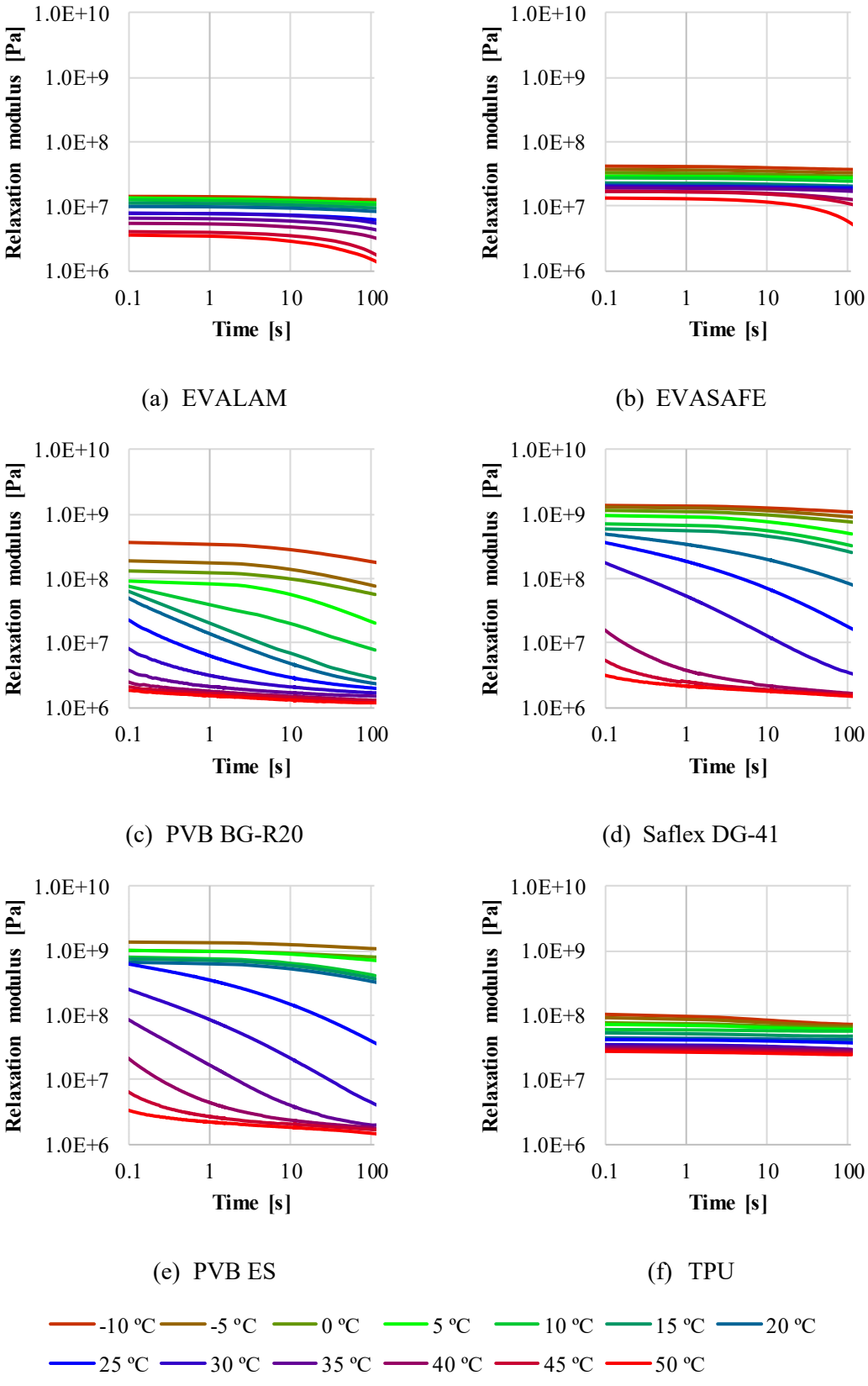

Figure 8. Relaxation curves of six different interlayer materials at different temperatures.

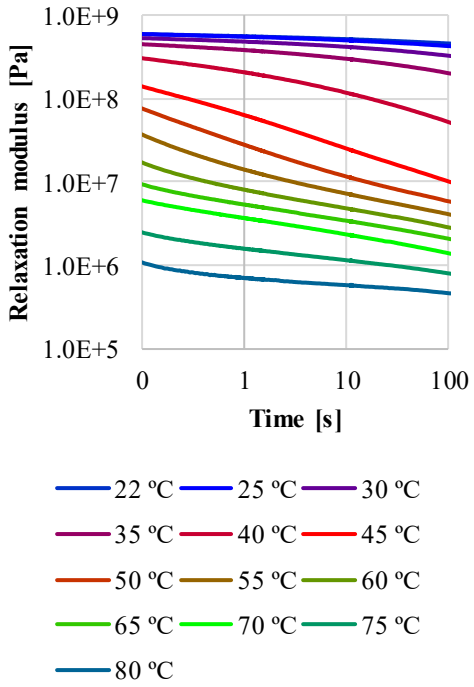

Figure 9. Relaxation curves of SentryGlas at different temperatures.

As SentryGlas presents a higher glass transition temperature, its glassy plateau zone is observed at higher temperatures than in the other materials being approximately for 20-22 ºC. From the relaxation curves at different temperatures, applying the WLF time-temperature superposition [13] by using the CFS algorithm developed by Gergesova et al. [14], it was possible to obtain the overlay curve. The coefficients C_1 and C_2 for the WLF TTS model, which allows obtaining the shift factors a_T for each isothermal relaxation curve, are listed in Table 2. The C_1 and C_2 constants were obtained by means of fitting the experimental a_T obtained from the CFS overlay curve with the WLF model; which could imply certain errors for the whole range of temperatures tested [6].

Table 2. WLF coefficients (C1 and C2) of each tested interlayer material applied to obtain the shift factors a_T.

Material	**C_1**	**C_2**
EVALAM	13.261	52.604
EVASAFE	33.492	130.94
PVB BG-R20	17.495	105.26
Saflex DG-41	17.899	85.08
PVB ES	31.483	170.32
TPU	125.58	364.46
SentryGlas	26.53	62.77

The master curves for each interlayer were obtained from these overlay curves, and they are presented in Figure 10. All master curves are placed in the same diagram in Figure 11. The reference temperature was the same for all interlayer materials in order to simplify the subsequent comparative study. The chosen reference temperature was 20 ºC, as it was considered a typical temperature in buildings, especially for indoor applications.

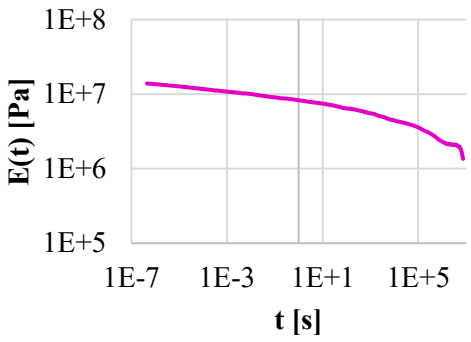

(a) EVALAM

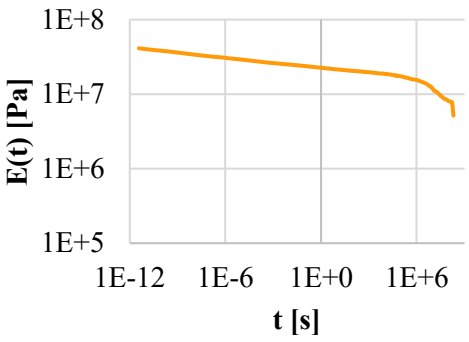

(b) EVASAFE

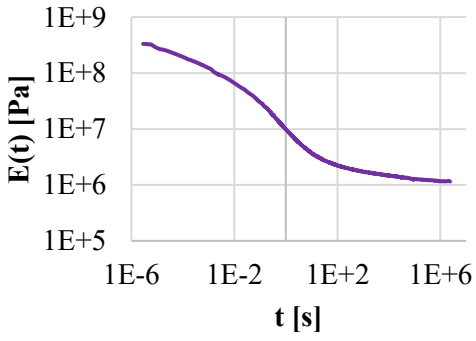

(c) PVB BG-R20

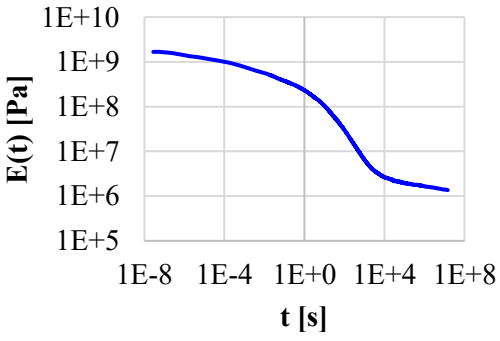

(d) Saflex DG-41

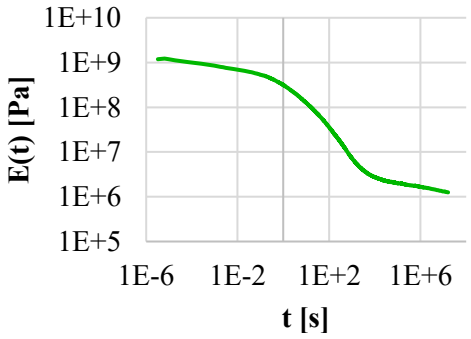

(e) PVB ES

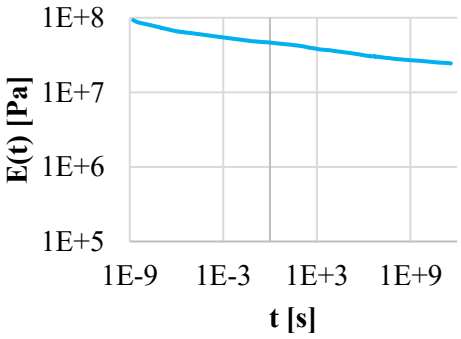

(f) TPU

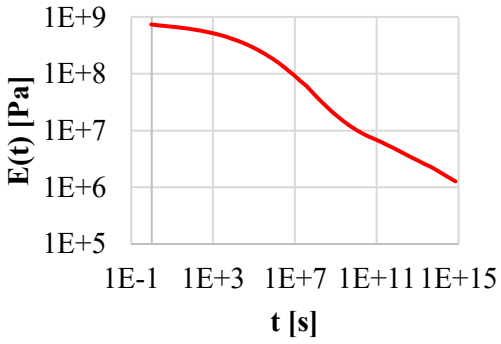

(g) SentryGlas

Figure 10. Relaxation master curves (E(t)) of the 7 tested polymeric interlayer materials separately (reference temperature: 20 ºC).

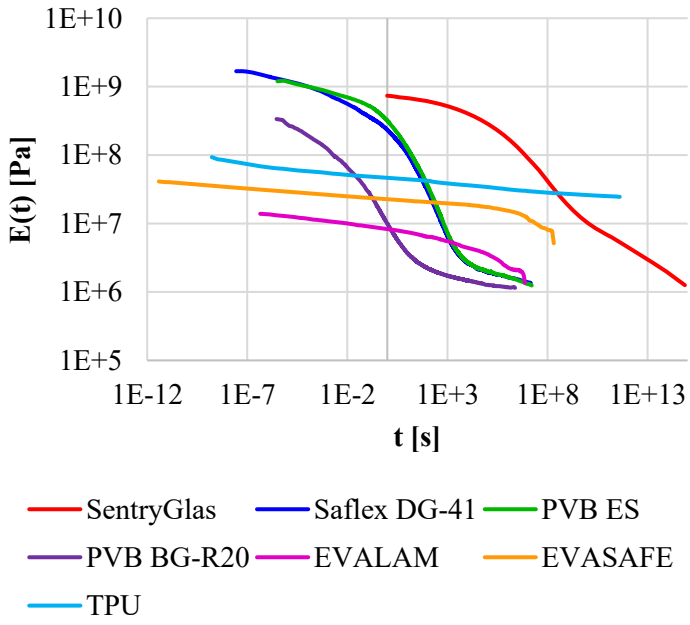

Figure 11. Relaxation master curves (E(t)) of the seven tested polymeric interlayer materials (reference temperature: 20 ºC).

According to these results, EVASAFE and EVALAM presented similar relaxation rates, but EVASAFE was stiffer in the tested time and temperature range. None of these two curves included the glass transition, since it happened below -10 ºC [32]. On the other hand, both EVA presented a drop of the Young modulus value at the higher tested temperatures, which may be because EVA has a secondary crystallization at about 43.7 ºC [33], during which the polymer chains are prone to change [34]. If that was the case, the polymer would lose its thermorheological simplicity. The way this affects the material response might be seen at higher temperatures. However, for temperatures above 50 ºC the material softened to such an extent that the film slipped from the clamp, which led to errors in the readings. TPU presented a similar relaxation rate as EVASAFE but was approximately twice as stiff and did not experience a stiffness drop in the tested time and temperature ranges.

The relaxation master curves of PVB ES and Saflex DG-41 were very close to overlapping: they had similar values of E_0, T_g, and E_∞. As expected, PVB BG-R20 had lower values of E_0 and T_g than PVB ES and Saflex DG-41, since it had a higher amount of plasticiser. On the other hand, SentryGlas had a lower E_0 than PVB ES and Saflex DG-41, but higher than PVB BG-R20 and had the highest T_g of all tested interlayers.

To model the experimental viscoelastic behaviour, a generalized Maxwell model, represented by a Prony series, was applied to fit the experimental relaxation master curve for each tested material. The Prony coefficients are presented in Table 3 for the different tested polymers. Each model had 13 Maxwell terms, except the EVALAM and SentryGlas models, which had 12 each. In all cases, the r^2 value was higher than 0.99, which means that the models fit properly the experimental curves. It is necessary to use all the presented decimals for each coefficient in order to avoid accumulating rounding errors.

Table 3. Coefficients of the Prony series for the fit equations of the relaxation master curves.

Coef.	EVALAM	EVASAFE	PVB BG-R20	Saflex DG-41	PVB ES	SentryGlas	TPU
E_0	1.39269E+07 Pa	4.12330E+07 Pa	3.34828E+08 Pa	1.68627E+09 Pa	1.19458E+09 Pa	7.3635968E+08 Pa	8.69630E+07 Pa
r^2	0.99978	0.99934	0.99919	0.99978	0.99983	0.99988	0.99655
τ_i	5.601263211047950E-06	1.242405743346480E-10	2.373007148117920E-05	3.796133763347350E-07	3.064386882064190E-05	1.332378306000000E+01	1.191003131603740E-07
	7.093447622251160E-05	4.089854746749950E-09	1.957885470727660E-04	5.140043760247610E-06	2.904824084163210E-04	1.857425850000000E+02	4.167708299561080E-06
	8.983152062980280E-04	1.346332463375320E-07	1.615383046581530E-03	6.959725737894970E-05	2.753569730154570E-03	2.589359724000000E+03	1.458417027572480E-04
	1.137627642917840E-02	4.431969383212600E-06	1.332796236652800E-02	9.423612834063520E-04	2.610191198895830E-02	3.609796680000000E+04	5.103476715338590E-03
	1.440693249827300E-01	1.458952610003140E-04	1.099643711251620E-01	1.275976700673650E-02	2.474278395851920E-01	5.032400940000000E+05	1.785872908200730E-01
	1.824495961415260E+00	4.802701765714990E-03	9.072776906484070E-01	1.727698887179300E-01	2.345442580133350E+00	7.015551480000000E+06	6.249351612910610E+00
	2.310544256120870E+01	1.580993384723590E-01	7.485631932650180E+00	2.339340086056970E+00	2.223315252610640E+01	9.779977620000000E+07	2.186851897604300E+02
	2.926076501343410E+02	5.204445756726370E+00	6.176133945392770E+01	3.167514940735780E+01	2.107547101924820E+02	1.363401774000000E+09	7.652507841254560E+03
	3.705587403934240E+03	1.713242819130620E+02	5.095712807499510E+02	4.288880851306930E+02	1.997807005379090E+03	1.900699416000000E+10	2.677862013637780E+05
	4.692761109250510E+04	5.639795464308750E+03	4.204294991996530E+03	5.807233525608650E+03	1.893781081854140E+04	2.649699990000000E+11	9.370712337497670E+06
	5.942919280520290E+05	1.856554863330930E+05	3.468817228810990E+04	7.863114502394470E+04	1.795171794038290E+05	3.693878622000000E+12	3.279117791168180E+08
	7.526121350000000E+06	6.111561992576990E+06	2.862000166449280E+05	1.064681993674190E+06	1.701697097404460E+06	5.149592280000000E+13	1.147470235035200E+10
	---	2.011854900000000E+08	2.361336562999990E+06	1.441601476500000E+07	1.613089633499990E+07	7.179012540000000E+14	4.015372500000000E+11
e_i	8.934652372544430E-02	1.145928897537480E-01	3.349286577163660E-01	1.378866241496520E-01	1.219115648996510E-01	1.218800000000000E-01	2.288847122942530E-01
	7.999961286124850E-02	6.292580693752550E-02	1.996516511049210E-01	1.502746856734460E-01	1.267824386332000E-01	1.095300000000000E-01	6.035254534298860E-02
	6.594879925044020E-02	6.260126882204320E-02	2.010696962772720E-01	1.293415723905710E-01	1.356375153549300E-01	1.725800000000000E-01	6.876311437396340E-02
	7.174497396363950E-02	5.717304165146200E-02	1.117539016851200E-01	1.673882322438900E-01	9.505680903242170E-02	1.910400000000000E-01	6.657974200002590E-02
	6.784243108881990E-02	6.025669055167680E-02	9.427615501995990E-02	1.391400878096740E-01	1.841922849876080E-01	1.786800000000000E-01	3.322616255654690E-02
	5.758528371221260E-02	3.687723123712640E-02	3.949697297278780E-02	1.007415433273280E-01	1.963552037104450E-01	1.262300000000000E-01	3.779183021339990E-02
	8.240878057237180E-02	4.782908207367090E-02	9.570357291904500E-03	1.008655089862080E-01	9.970535661917730E-02	6.270400000000000E-02	5.958338022339350E-02
	6.757672312105960E-02	4.166751071277870E-02	2.918894829862710E-03	5.920922290910070E-02	3.255900794072450E-02	2.052800000000000E-02	3.856755273784410E-02
	9.429271408639160E-02	3.170938074605540E-02	1.186318753376010E-03	1.249437916730990E-02	5.446209565293200E-03	6.534200000000000E-03	4.229244728388130E-02
	6.159023954029160E-02	3.522502610377670E-02	6.545949951796980E-04	1.240940691866310E-03	4.752536180737180E-04	3.597100000000000E-03	3.192508456571670E-02
	1.060623436614500E-01	5.194540401782030E-02	6.404409634312020E-04	3.228586865337250E-04	3.804958695469180E-04	2.646900000000000E-03	2.122210363960120E-02
	4.302348055028850E-02	1.285313606359310E-01	2.958003009124670E-04	1.376532248184410E-04	1.716780564775720E-04	1.497500000000000E-03	1.801897692912610E-02
	---	1.880675480987830E-01	1.821659289080540E-04	2.686429657412980E-04	4.922182074167310E-04	1.372400000000000E-03	1.866291343779040E-02

With these Prony coefficients, it was possible to calculate the dynamic master curves for the reference temperature of 50 ºC, presented in Figure 12. Knowing the variation of E' and E'' with frequency can be useful during the service life of the material, especially in applications where dynamic loading (e.g. wind, seismic, and pedestrian) is expected. That is, however, still taking into account that the material properties of the film alone may differ from the ones after the lamination process [5].

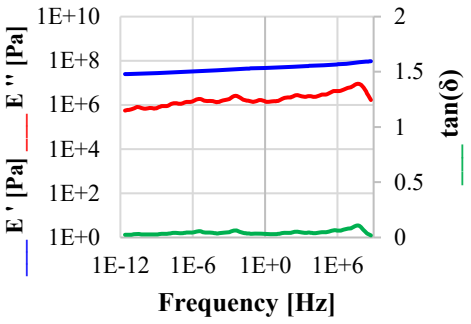

(a) TPU

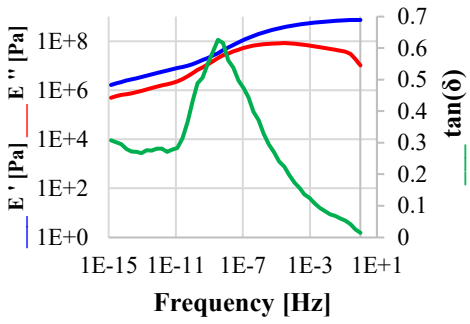

(b) SentryGlas

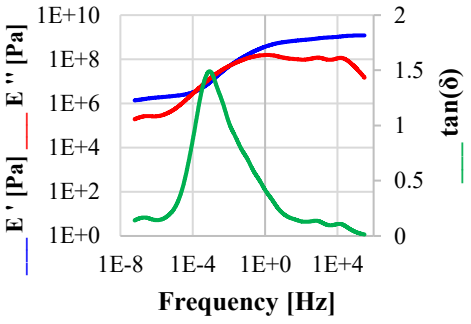

(c) PVB ES

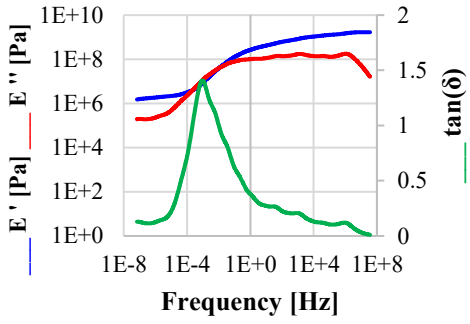

(d) Saflex DG-41

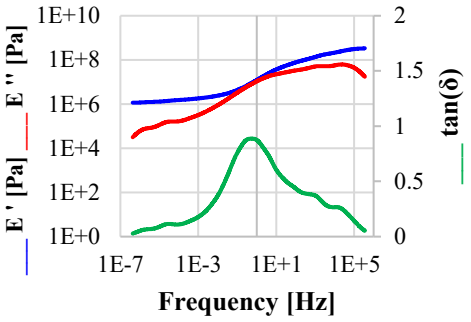

(e) PVB BG-R20

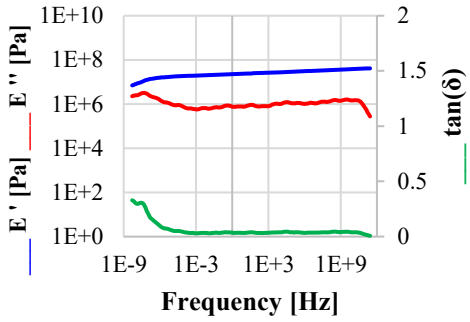

(f) EVASAFE

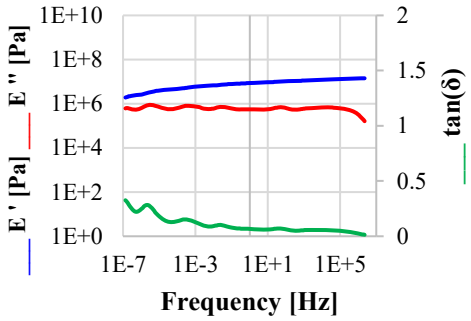

(g) EVALAM

Figure 12. Dynamic master curves (E'(ω) and E''(ω)) of the seven tested polymeric interlayer materials (reference temperature: 20 ºC).

For TPU, EVALAM, and EVASAFE, the value of the storage modulus increases gradually over frequency, but it increases less than one order of magnitude in all three cases. The dynamic master curves of PVB ES and Saflex DG-41 present a very similar behaviour: in both cases E' and E'' increase with frequency. In addition to that, E' has a higher value than E'' for almost all frequencies, except near 40-45 Hz, where E'' is slightly higher than E', meaning that the viscous component is more predominant at this frequency range. Something similar happens with PVB BG-R20, but in this case E'' has a higher value than E' at a much higher frequency of approximately 4100 Hz. In the case of SentryGlas, E' and E'' also increase over frequency, but in this case E' is always above E'', meaning that it has a more elastic and less viscous response than any of the previously mentioned PVB. It is at a frequency of approximately 0.3 Hz that E'' approaches E' the most. The exact frequency values are not as important as the overall tendency and the comparison between materials, because the first is different for each reference temperature.

The ratio between the loss modulus and the storage modulus, here presented as tan(δ), also provides relevant information. A peak in tan(δ) indicates the region in which the loss modulus, associated to the viscous part of the material, has a higher contribution, and may correspond to the glass transition (T_g) region [6]. The coefficient tan(δ) is also used as a reference of the damping coefficient, which is commonly used in laminated glass for acoustic insulation or vibration reduction. In this case, the low value of tan(δ) presented by EVA and TPU indicate that these will have a lower damping than PVB. SentryGlas would be in an intermediate value between both groups.

PVB samples and SentryGlas have a local maximum of tan(δ) within the range presented in the diagrams, but with different values and for different frequencies (Table 4): the higher the T_g, the lower the frequency at which the peak is presented, and the higher the E_0, the higher the peak value of tan(δ). No visible tendency is observed in the case of TPU, where the value oscillates between 0.1 and 0, meaning that the material has a predominantly elastic behaviour. In the case of EVA, tan(δ) gradually decreases over frequency, starting near 0.35 and finishing near 0. The fact that TPU and EVA do not have a clear peak value of tan(δ) confirms that these materials did not experience glass transition in the tested range.

Table 4. Peak value of tan(δ) and frequency at which it occurs in the presented dynamic master curves (reference temperature: 50 ºC).

Material	**SentryGlas**	**PVB ES**	**Saflex DG-41**	**PVB BG-R20**
tan(δ)	0.718	1.49	1.41	0.863
Frequency	0.32592 Hz	44.424 Hz	42.981 Hz	4103.2 Hz

5. Conclusions

Relaxation tests at different temperatures were performed on seven polymeric films used as interlayer materials for laminated glass: EVALAM, EVASAFE, PVB BG-R20, Saflex DG-41, PVB ES, SentryGlas, and TPU. From the relaxation curves at different temperatures, it was possible to build the relaxation master curve using the t-T-P shifting (CFS) algorithm [14]. An equation to fit each relaxation master curve was then obtained using a generalized Maxwell model [6], and the Prony coefficients of each model were presented. Finally, the dynamic master curve of each interlayer material was obtained by using interconversion methods [6,16,17].

The mechanical properties obtained for the seven polymers studied in this paper, which are used as an interlayer for laminated glass, can be used to predict the flexural behaviour of laminated glass elements under static and dynamic loading. The numerical model to define the viscoelastic behaviour of these seven materials was considered in terms of the Prony series (Eq. 10), with the coefficients E_0, e_i, and τ_i presented in Table 3.

The relaxation master curves show how the stiffness of all tested materials decreases over time, but at different rates: TPU and EVA were less sensitive to load duration and temperature variations. The stiffness of both EVA polymers started decreasing at a higher rate for higher temperatures within the tested range because the materials experienced a secondary crystallization. The T_g of TPU and EVA is below -10 ºC [18], and therefore for these materials the temperature during the relaxation tests was always above T_g. Instead, the T_g of PVB and SentryGlas was within the temperature range of the relaxation tests.

The glass transition region can be associated to a drop of the stiffness in the relaxation master curves or a peak value in the tan(δ) value of the dynamic master curves. According to both, SentryGlas presented the highest T_g of all the tested interlayer materials. The T_g of stiff PVB is higher than the one of standard PVB (PVB BG-R20). There were no significant differences between PVB ES and Saflex DG-41, which are materials with similar properties from different manufacturers.

The dynamic master curves show how the storage modulus of all tested interlayer materials increases with frequency, and it increases at a higher rate for PVB and SentryGlas than for TPU and EVA. TPU and EVA have lower values of tan(δ), which is associated to the damping coefficient commonly used for acoustic insulation and vibration reduction of laminated glass.

Acknowledgements

The work was partially funded by CRISTEC with CDTI funds (IDI-20160588). The authors would like to thank the Catalan Government for the quality accreditation given to their research groups GREiA (2017 SGR 1537) and DIOPMA (2017 SGR 0118). GREiA and DIOPMA are certified agents TECNIO in the category of technology developers from the Government of Catalonia. This work is partially supported by ICREA under the ICREA Academia programme. The financing support given by the Spanish Ministry of Economy and Competitiveness through the project DPI2016-80389-C2-2-R is gratefully appreciated. Xavier Centelles would like to thank University of Lleida for his research fellowship and to the University of Oviedo for hosting his secondment during 2019.

References

1. M. López-Aenlle, F. Pelayo. Static and dynamic effective thickness in five-layered glass plates. Composite Structures 212 (2019) 259-270. https://doi.org/10.1016/j.compstruct.2019.01.037
2. D. Baraldi, A. Cecchi, P. Foraboschi. Broken tempered laminated glass: Non-linear discrete element modelling. Composite Structures 140 (2016) 278–295. http://dx.doi.org/10.1016/j.compstruct.2015.12.050
3. L. Biolzi, S. Cattaneo, M. Orlando, L.R. Piscitelli, P. Spinelli. Post-failure behavior of laminated glass beams using different interlayers. Composite Structures 202 (2018) 578–589. https://doi.org/10.1016/j.compstruct.2018.03.009
4. L. Biolzi, M. Orlando, L.R. Piscitelli, P. Spinelli. Static and dynamic response of progressively damaged ionoplast laminated glass beams. Composite Structures 157 (2016) 337–347. http://dx.doi.org/10.1016/j.compstruct.2016.09.004
5. M. López-Aenlle, A. Noriega, F. Pelayo. Mechanical characterization of polyvinil butyral from static and modal tests on laminated glass beams. Composites Part B 169 (2019) 9–18. https://doi.org/10.1016/j.compositesb.2019.03.077
6. F. Pelayo, M.J. Lamela-Rey, M. Muniz-Calvente, M. López-Aenlle, A. Álvarez-Vázquez, A. Fernández-Canteli. Study of the time-temperature-dependent behaviour of PVB: Application

to laminated glass elements. Thin-Walled Structures 119 (2017) 324–331. http://dx.doi.org/10.1016/j.tws.2017.06.030

7. L. Andreozzi, S.B. Bati, M. Fagone, G. Ranocchiai, F. Zulli. Dynamic torsion tests to characterize the thermo-viscoelastic properties of polymeric interlayers for laminated glass. Construction and Building Materials 65 (2014) 1–13. http://dx.doi.org/10.1016/j.conbuildmat.2014.04.003
8. T. Serafinavičius, J.-P. Lebet, C. Louter, T. Lenkimas, A. Kuranovas. Long-term laminated glass four point bending test with PVB, EVA and SG interlayers at different temperatures. Procedia Engineering 57 (2013) 996–1004. doi: https://doi.org/10.1016/j.proeng.2013.04.126
9. M. López-Aenlle, F. Pelayo. Dynamic effective thickness in laminated-glass beams and plates. Composites: Part B 67 (2014) 332–347. http://dx.doi.org/10.1016/j.compositesb.2014.07.018
10. G. Ranocchiai, F. Zulli, L. Andreozzi, M. Fagone. Test Methods for the Determination of Interlayer Properties in Laminated Glass. Journal of Materials in Civil Engineering 29 (2017) 04016268. https://doi.org/10.1061/(ASCE)MT.1943-5533.0001802
11. J.D. Ferry. Viscoelastic Properties of Polymers. John Wiley & Sons, New York (1980). ISBN: 978-0-471-04894-7
12. M. Overend, Q. Jin, J. Watson. The selection and performance of adhesives for a steel–glass connection. International Journal of Adhesion and Adhesives 31 (2011) 587-597. https://doi.org/10.1016/j.ijadhadh.2011.06.001
13. M.L. Williams, R.F. Landel, J. Ferry. The temperature dependence of relaxation mechanisms in amorphous polymers and other glass-forming liquids. Journal of the American Chemical Society 77 (1955)3701-3707 https://doi.org/10.1021/ja01619a008
14. M. Gergesova, B. Zupančič, I. Saprunov, I. Emri. The closed form t-T-P shifting (CFS) algorithm. Journal of Rheology 55 (2011) 1-16. https://doi.org/10.1122/1.3503529
15. International Organization for Standardization. (2017). Mechanical vibration and shock - Characterization of the dynamic mechanical properties of visco-elastic materials - Part 6: Time-temperature superposition (ISO 18437-6)
16. S.W. Park, R.A. Schapery. Methods of interconversion between linear viscoelastic material functions. Part I – a numerical method based on Prony series. International Journal of Solids and Structures 25 (1999) 1653-1675. https://doi.org/10.1016/S0020-7683(98)00055-9
17. I. Emri, B.S. von Bernstorff, R. Cvelbar, A. Nikonov. Re-examination of the approximate methods for interconversion between frequency- and time-dependent material functions. J. Non-Newtonian Fluid Mech. 129 (2005) 75–84. https://doi.org/10.1016/j.jnnfm.2005.05.008
18. M. Martín, X. Centelles, A. Solé, C. Barreneche, A.I. Fernández, L.F. Cabeza. Polymeric interlayer materials for laminated glass: A review. Construction and Building Materials 230 (2020) 116897. https://doi.org/10.1016/j.conbuildmat.2019.116897

19. S. Chen, M. Zang, D. Wang, S. Yoshimura, T. Yamada. Numerical analysis of impact failure of automotive laminated glass: A review. Composites Part B: Engineering 122 (2017) 47-60. https://doi.org/10.1016/j.compositesb.2017.04.007
20. M.A. Samieian, D. Cormie, D. Smith, W. Wholey, B.R.K. Blackman, J.P. Dear, P.A. Hooper. On the bonding between glass and PVB in laminated glass. Engineering Fracture Mechanics 214 (2019) 504-519. https://doi.org/10.1016/j.engfracmech.2019.04.006
21. Y. Shitanoki, S.J. Bennison, Y. Koike. Structural behavior thin glass ionomer laminates with optimized specific strength and stiffness. Composite Structures 125 (2015) 615-620. https://doi.org/10.1016/j.compstruct.2015.02.013
22. R. Couderc, M. Amara, J. Degoulange, F. Madon, R. Einhaus. Encapsulant for glass-glass PV modules for minimum optical losses: gas or EVA? Energy Procedia 124 (2017) 470-477. https://doi.org/10.1016/j.egypro.2017.09.283
23. A. Rühl, S. Kolling, J. Schneider. Characterization and modeling of poly(methyl methacrylate) and thermoplastic polyurethane for the application in laminated setups. Mechanics of Materials 113 (2017) 102-111. https://doi.org/10.1016/j.mechmat.2017.07.018
24. Hornos Industriales Pujol, S.A. (2016). Catálogo Evalam
25. Bridgestone (2016). The glass experience – Films de inserción
26. Kuraray (2016). Trosifol Architectural laminated glass interlayers
27. Eastman Chemical Company (2015). Product Information Bulletin - Saflex DG Structural Interlayer
28. C. Louter, J. Belis F. Veer, J.-P. Lebet. Structural response of SG-laminated reinforced glass beams; experimental investigations on the effects of glass type, reinforcement percentage and beam size. Engineering Structures 36 (2012) 292-301. https://doi.org/10.1016/j.engstruct.2011.12.016
29. M. Santarsiero, C. Bedon, C. Louter. Experimental and numerical analysis of thick embedded laminated glass connections. Composite Structures 188 (2018) 242-256. https://doi.org/10.1016/j.compstruct.2018.01.002
30. J.E. Minor (2009) Architectural Glass to Resist Seismic and Extreme Climatic Events. Chapter 8: Glazing systems to resist windstorms on special buildings. Woodhead Publishing Series in Civil and Structural Engineering. https://doi.org/10.1533/9781845696856.217
31. X. Centelles, M. Martín, A. Solé, J.R. Castro, L.F. Cabeza. Tensile test on interlayer materials for laminated glass under diverse ageing conditions and strain rates. Construction and Building Materials 243 (2020) 118230. https://doi.org/10.1016/j.conbuildmat.2020.118230
32. K. Agroui, G. Collins, J. Farenc. Measurement of glass transition temperature of crosslinked EVA encapsulant by thermal analysis for photovoltaic application. Renewable Energy 43 (2012) 218-223. https://doi.org/10.1016/j.renene.2011.11.015

33. S. Chen, J. Zhang, J. Su. Effect of Damp-Heat Aging on the Properties of Ethylene-Vinyl Acetate Copolymer and Ethylene-Acrylic Acid Copolymer Blends. Journal of Applied Polymer Science 114 (2009) 3110 – 3117. https://doi.org/10.1002/app.30859
34. S. Chen, J. Zhang, J. Su. Effect of Hot Air Aging on the Properties of Ethylene-Vinyl Acetate Copolymer and Ethylene-Acrylic Acid Copolymer Blends. Journal of Applied Polymer Science 112 (2009) 1166-1174. https://doi.org/10.1002/app.29506